

Van der Waals Complexes between Boron Trifluoride and Carbon Monoxide: A Theoretical Study

V. M. Rayón and J. A. Sordo*

Departamento de Química Física y Analítica, Facultad de Química, Universidad de Oviedo, Julián Clavería 8, 33006 Oviedo, Principado de Asturias, Spain

Received: April 15, 1997[⊗]

An *ab initio* study on the 1:1 and 1:2 van der Waals complexes between boron trifluoride and carbon monoxide has been carried out. Full geometry optimizations are performed at the MP2/6-31G* and MP2/D95* levels. The bond energies computed at different levels (MP2, MP4) and with several basis sets (6-31G*, D95*, and aug-cc-pVDZ) range from 3.2 to 3.5 kcal/mol for $\text{BF}_3 \cdots \text{CO}$ and from 6.4 to 6.6 kcal/mol for $\text{OC} \cdots \text{BF}_3 \cdots \text{CO}$. The *counterpoise*-corrected values range from 0.7 to 1.6 kcal/mol for $\text{BF}_3 \cdots \text{CO}$ and from 1.3 to 3.1 kcal/mol for $\text{OC} \cdots \text{BF}_3 \cdots \text{CO}$. These (gas phase) computed values are consistent with the corresponding experimental dissociation enthalpies as measured in liquefied argon (1.8 and 3.5 kcal/mol). The MP2/6-31G* computed vibrational frequencies agree quite well with the infrared measurements. The analysis of the frequencies together with the energetic data gives theoretical support to some tentative assignments proposed in the infrared studies. The experimental suggestion about the formation of the never observed before $\text{BF}_3 \cdots \text{OC}$ and $\text{OC} \cdots \text{BF}_3 \cdots \text{CO}$ adducts is theoretically confirmed. A theoretical analysis of the wave functions shows that the weakness of the complexes formed can be ascribed to the small charge transfer detected.

Introduction

The recent literature shows an impressive growth of the number of papers dealing with weakly bound complexes using both experimental and theoretical tools.¹ Such an interest is directly related to the fact that the findings serve to explore, at the molecular level, the nature of the interactions involved when passing from gas phase chemistry to condensed phase chemistry, a subject of relevance in a number of areas of chemistry, physics, and biology.

Boron trifluoride is a weak Lewis acid and carbon monoxide is a poor σ donor. As a consequence, the formation of adducts of the type $\text{BF}_3(\text{CO})_n$ is not at all a trivial task from the experimental viewpoint. Molecular beam electric resonance spectroscopy² and infrared studies³ carried out under nonequilibrium conditions provided structural parameters (B–C bond length and C–B–F angle) for the $\text{BF}_3 \cdots \text{CO}$ complex which agreed quite well with *ab initio* predictions.⁴

In order to obtain more complete information on the interaction between BF_3 and CO, cryogenic solutions to form van der Waals complexes under equilibrium conditions were analyzed in a very recent experimental study where the infrared spectra of solutions in liquefied argon (85–115 K) containing both boron trifluoride and carbon monoxide have been reported.⁵ Using concentration variations, bands due to the 1:1 complex $\text{BF}_3 \cdots \text{CO}$ and to a 1:2 $\text{BF}_3(\text{CO})_2$ complex were identified, and from temperature-dependent studies the dissociation enthalpies of such complexes were found to be 1.8 and 3.5 kcal/mol, respectively. A very weak band is tentatively assigned by the authors to the 1:1 complex $\text{BF}_3 \cdots \text{OC}$ in which carbon monoxide is binding to the boron atom via its oxygen atom.

In this paper we present a theoretical analysis with the aim of complementing the experimental study carried out by van der Veken and Sluyts.⁵ Our results provide theoretical support for some of the hypotheses put forward by these authors regarding the characteristics of the complexes formed in $\text{BF}_3/$

CO mixtures, allowing for the analysis, on a theoretical basis, of the nature of the interactions involved.

Methods

Ab initio calculations at the MP4(SDTQ)/6-31G**/MP2/6-31G* level were carried out to explore the interaction energy hypersurfaces corresponding to the $\text{BF}_3(\text{CO})_n$ ($n = 1, 2$) van der Waals complexes. Although this level of theory has proved appropriate to provide reliable information on this type of system,^{4,6–8} we have analyzed the basis set effect on the computed bond energies in the present case by using additional bases from different laboratories (besides Pople's 6-31G* basis set,^{9a} Dunning's contraction [4s,2p,1d]^{9b} (polarized full double- ζ) from Huzinaga's (9s,5p) basis set,^{9c} D95*, and Dunning's augmented correlation-consistent polarized valence double- ζ basis set, aug-cc-pVDZ^{9d} were used to compute the most significant structures). It is clear that the use of different basis sets, generated from quite dissimilar strategies¹⁰ and rendering similar results, does provide additional support to the validity of the conclusions reached in any *ab initio* study. Harmonic frequencies (at the MP2/6-31G* level) confirmed that reactants and minima have no imaginary frequencies, while transition structures have one. The *counterpoise* method (CP)¹¹ was used to correct the interaction energies for the basis set superposition error (BSSE), which is known to be appreciable in calculations on van der Waals systems using Pople's split-valence 6-31G basis sets.¹² Fragment relaxation energy terms were taken into account in the estimation of the BSSE.¹³ All the calculations were carried out with the GAUSSIAN 92 and 94 packages of programs.¹⁴

The NEDA (natural energy decomposition analysis)¹⁵ partitioning scheme (electrostatic, charge transfer, and deformation components) was used to estimate the relative importance of charge transfer and electrostatic interactions in the van der Waals complexes studied.

In order to throw some light on the important problem¹⁶ of the nature of the interactions involved in the type of systems studied, their wave functions were analyzed by means of a

[⊗] Abstract published in *Advance ACS Abstracts*, August 15, 1997.

recently developed methodology,¹⁷ based on the expansions of the MOs of a complex system in terms of the MOs of its fragments, using the geometry each fragment has in the complex, and the performance of the configurational analysis. Such a method was originally developed by Fukui's group for bimolecular interactions¹⁸ and extended by us to three-molecule interactions.¹⁷

The basic ideas of the method can be summarized as follows: Let us consider three species A, B, and C and their composite system A–B–C. We represent the MOs of A–B–C, ψ_g ($g = 1, 2, \dots, \text{occ}$), by linear combinations of the MOs of A, B, and C as

$$\psi_g = \sum_{i=1}^{\text{occ}} D_i(g) a_i + \sum_{j=1}^{\text{unocc}} D_j(g) a_j + \sum_{k=1}^{\text{occ}} D_k(g) b_k + \sum_{l=1}^{\text{unocc}} D_l(g) b_l + \sum_{m=1}^{\text{occ}} D_m(g) c_m + \sum_{n=1}^{\text{unocc}} D_n(g) c_n \quad (1)$$

where a_i , b_k , and c_m refer to the occupied MOs of systems A, B, and C, respectively, and a_j , b_l , and c_n to the corresponding unoccupied MOs.

A calculation on the composite system A–B–C and on A, B, and C, separately, renders the MOs ψ and a , b , and c in terms of the atomic basis functions used to compute A, B, and C. Then the coefficients $D_i(g)$, $D_j(g)$, ..., $D_n(g)$ in eq 1 can be obtained by solving linear simultaneous equations to fit the basis functions coefficients with respect to each MO of A–B–C.

To express the wave function of the complex, Ψ , in a chemically graspable form, we rewrite it by combination of various electronic configurations as

$$\Psi = c_0 \Psi_0 + \sum_q c_q \Psi_q \quad (2)$$

where Ψ_0 is the state in which neither electron transfer nor electron excitation takes place and Ψ_q stands for monotruncated configurations (one electron in an occupied MO in any of the three fragments A, B, and C is transferred to an unoccupied MO of a different fragment), monoexcited configurations (one electron in an occupied MO of any of the three fragments A, B, and C is excited to an unoccupied MO of the same fragment), etc. The coefficients c_0 and c_q in eq 2 are computed by means of mathematical expressions previously derived.¹⁷ This method has proved useful for understanding the chemical features of complex formation in quite different systems,¹⁹ being especially suited for studying weakly bound complexes.²⁰

Results and Discussion

Two minima were located in the case of the 1:1 type of complexes (**1**, **2**; both C_{3v}) and four transition structures connecting them (see Figures 1 and 2): **TS1**(**1**→**1'**), **TS2**(**2**→**2'**), **TS3**(**1**→**2**), and **TS4**(**1**→**2'**) (**1'** and **2'** are equivalent to **1** and **2**, respectively, with the CO molecule at different positions in relation to the BF₃ molecule: upper (**1**, **2**) and lower (**1'**, **2'**); see Figure 1). As expected (see previous section and references quoted therein) the computed geometrical parameters are in good agreement with the experimental values available. Indeed, in the case of the BF₃⋯CO (**1**) complex the resulting B⋯C distance and CBF angle are 2.771 (2.819) Å and 91.4° (91.4)°, respectively, as computed at the MP2/6-31G* (MP2/D95*) level, which agree quite well with the experimental values 2.886(5) Å and 90.65(25)° reported in ref 2. Seven minima were located in the case of the 1:2 type of complexes (**3**, **4** D_{3h} , **5** C_{3v} , and

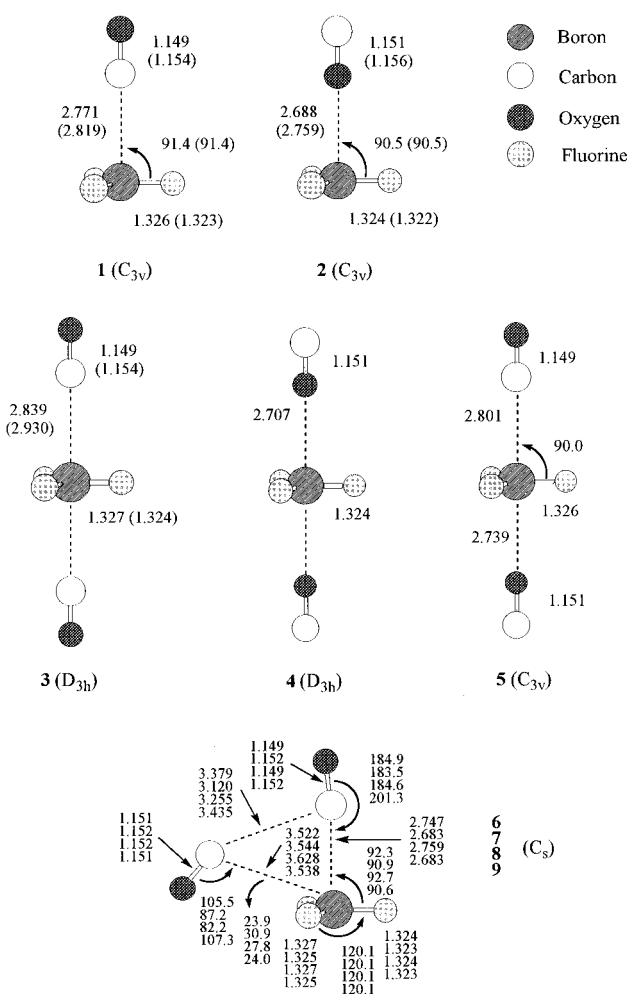


Figure 1. 1:1 and 1:2 stable structures (minima) located at the MP2/6-31G* and MP2/D95* (values in parentheses) levels for the interaction between boron trifluoride and carbon monoxide. Distances are given in angstroms and angles in degrees.

6–9 C_s ; see Figure 1). In that case, the search for transition structures connecting the minima was not undertaken because their analysis is beyond the scope of the present paper. Table 1 collects the calculated bond energies for the structures **1–9** depicted in Figures 1 and 2. Full geometry optimizations were carried out at the MP2/6-31G* level, and bond energies were computed at the MP4/6-31G**/MP2/6-31G* level for all nine structures **1–9**. The most significant structures **1–3** (see below) were also optimized at the MP2/D95* level, and the corresponding bond energies were computed at the MP2/aug-cc-pVDZ//MP2/D95* and MP4/D95**/MP2/D95* levels. The counterpoise-corrected values¹¹ including fragment relaxation terms¹³ are given in parentheses. The electron densities at the bond critical points according to a Bader type density analysis²¹ are also given for the structures **1–5** (the topology of the electron density of the structures **6–9** is notably more complex including a variety of bond, ring, and cage critical points). They show (the Laplacian of electron density, the ellipticity, and the sum of the potential and kinetic energy density at the bond critical points²¹ were also analyzed) that such structures correspond to van der Waals complexes. Table 2 contains the energy barriers (**TS1–TS4**) as computed in terms of differences in electronic energies (including or not the zero point energy correction), enthalpies, and free energies. (The energy barriers **TS1–TS4** are referred to the van der Waals minima **1** and **2**; therefore, no BSSE exists).²² Consequently, since all basis sets considered render rather similar uncorrected interaction

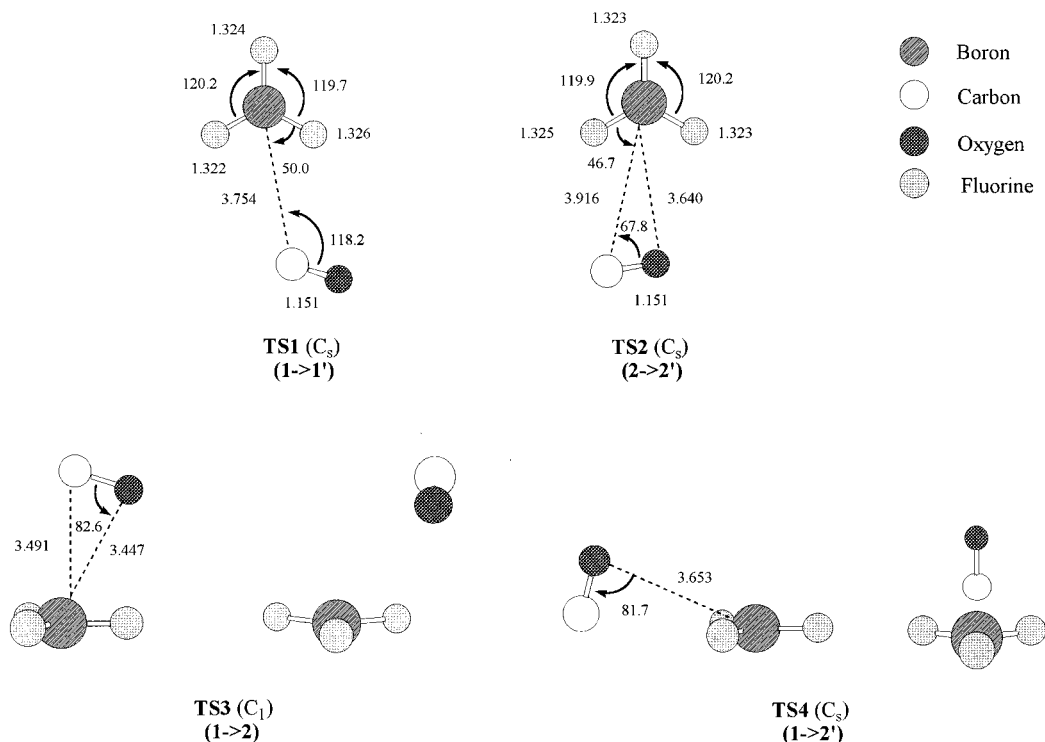


Figure 2. Transition structures located at the MP2/6-31G* level connecting the two C_{3v} 1:1 van der Waals complexes $\text{BF}_3 \cdots \text{CO}$ and $\text{BF}_3 \cdots \text{OC}$ (see Figure 1). $1'$ and $2'$ stand for the structures equivalent to **1** and **2** with the CO molecule in the plane below the BF_3 molecule according to C_{3v} symmetry. Distances are given in angstroms and angles in degrees.

TABLE 1: Calculated Bond Energies^a (kcal/mol) of the Nine Complexes Located (1–9): Dipole Moments (μ ; Computed at the MP2/6-31G* Level) Are Given in Debye and Electronic Density ($\rho(r_c)$), Computed at the Bond Critical Points, in au; Counterpoise-Corrected Values, Including Fragment Relaxation Terms, Are Given in Parentheses

		1	2	3	4	5	6	7	8	9	
ΔH	MP2/6-31G*	3.5	1.9	6.6	3.9	5.2	5.2	3.4	4.9	3.5	
		(1.0)	(0.3)	(1.9)	(0.6)	(1.2)	(0.8)	(-0.1)	(0.6)	(-0.1)	
	MP4/6-31G* ^b	3.5	2.2	6.6	4.3	5.4	5.2	3.7	4.9	3.8	
		(0.9)	(0.4)	(1.7)	(0.8)	(1.2)	(0.7)	(0.1)	(0.6)	(0.1)	
	MP2/D95*	3.5	2.0	6.6							
		(1.0)	(-0.1)	(1.9)							
μ	MP2/aug-cc-pVDZ ^c	3.5	2.1	6.4							
		(1.6)	(0.5)	(3.1)							
	MP4/D95* ^d	3.2	2.2	6.5							
		(0.7)	(0.2)	(1.3)							
$\rho(r_c)$	MP2/6-31G*	0.795	0.223	0.000	0.000	0.590	0.617	0.351	0.894	0.065	
		B–C	0.0114		0.0100		0.0107				
		B–O	0.0093		0.0090	0.0085					

^a Bond energies are computed by adding the correction for zero-point vibrational energies and the thermal correction to the enthalpy to the dissociation energies as given in ref 14 (it should be noted that only a part of the thermal correction to the enthalpy is considered in ref 4). Thermodynamic corrections are calculated at the MP2/6-31G* level in all cases. ^b MP4(SDTQ)/6-31G*/MP2/6-31G*. ^c MP4(SDQ)/D95*/MP2/D95*. ^d MP2/aug-cc-pVDZ//MP2/D95*.

energies—see Table 1—the cheapest one, 6-31G*, was chosen to compute the values presented in Table 2.) Table 3 collects the BF_3 symmetric stretching (ν_1), out-of-plane deformation (ν_2), BF_3 antisymmetric stretching (ν_3), and F–B–F bending (ν_4) MP2/6-31G* vibrational frequencies for the most relevant species.

Data collected in Tables 1 and 3 fully corroborate the assignments proposed by van der Veken and Sluyts in their experimental study.⁵ Indeed, the bond energies (with no consideration of BSSE) of the $\text{BF}_3 \cdots \text{CO}$ (**1**) and $\text{BF}_3 \cdots \text{OC}$ (**2**) complexes (see ΔH for structures **1** and **2** in Table 1) indicate that although **1** is more stable, **2** is also a stable structure with a bond energy close to that of **1** and it might well be experimentally detected. The experimental dissociation enthalpy for the $\text{BF}_3 \cdots \text{CO}$ complex as measured in liquefied argon⁵ (1.8 kcal/mol) is in between the theoretical (gas phase) uncorrected and CP-corrected values for all the theoretical levels employed.

This fact is consistent with the predicted overcorrection of the BSSE when using the CP method at the correlated level¹⁹ that makes some authors conclude in other studies on similar systems that for a comparison with experimental values directly calculated results should be used rather than estimated data obtained from correction procedures such as the CP method.⁴ In the present case, however, the experimental bond energy is closer to the CP-corrected values, especially at the MP2/aug-cc-pVDZ//MP2/D95* level of theory. On the other hand, the experimentally observed broad band on the low-frequency side of the out-of-plane deformation vibrational frequency of the monomer BF_3 ⁵ agrees quite well with the 685 cm^{-1} band reported in Table 3 for the $\text{BF}_3 \cdots \text{OC}$ (**2**) complex. Van der Veken and Sluyts comment that the formation of a weak complex like the 1:1 $\text{BF}_3 \cdots \text{OC}$ (**2**) one, in which the bonding occurs between the boron and the oxygen atoms, cannot greatly disturb the BF_3 modes, and consequently the band observed is situated closer

TABLE 2: MP2/6-31G* Inversion Barrier Heights (cm⁻¹; Referred to the Most Stable Complex Involved) As Computed in Terms of Differences in Electronic Energies, ΔE^\ddagger (Including or Not the Zero-Point Energy Corrections, ZPE), Enthalpies, ΔH^\ddagger , and Free Energies, ΔG^\ddagger (MP4(SDTQ)/6-31G//MP2/6-31G* Values in Parentheses)**

	ΔE^\ddagger	$\Delta E^\ddagger + \text{ZPE}$	ΔH^\ddagger	ΔG^\ddagger
TS1 ^a	1032 (1004)	911 (883)	939 (911)	683 (655)
TS2 ^b	447 (519)	394 (466)	372 (444)	255 (326)
TS3 ^c	1015 (994)	894 (873)	920 (899)	683 (661)
TS4 ^d	952 (920)	838 (807)	857 (826)	693 (662)

^a Transition structure connecting 1 and 1' structures (see the text and Figures 1 and 2). ^b Transition structure connecting 2 and 2' structures (see the text and Figures 1 and 2). ^c Transition structure connecting 1 and 2 structures (see the text and Figures 1 and 2). ^d Transition structure connecting 1 and 2' structures (see the text and Figures 1 and 2).

to the monomer band than those of the 1:1 BF₃⋯CO (**1**) and 1:2 OC⋯BF₃⋯CO (**3**) complexes.⁵ In full agreement with that argument, the MP2/6-31G* computed ν_2 band (685 cm⁻¹) for the BF₃⋯OC (**2**) complex (see Table 3) is closer to the corresponding ν_2 monomer band (699 cm⁻¹) than are the MP2/6-31G* computed ν_2 bands for BF₃⋯CO (**1**; 666 cm⁻¹) and OC⋯BF₃⋯CO (**3**; 645 cm⁻¹) complexes. On the other hand, the new weak band at 879 cm⁻¹ detected in the spectrum of mixed BF₃/CO solution⁵ (absent in the infrared spectrum of BF₃) correlates quite well with the MP2/6-31G* computed symmetric stretching band ν_1 of the BF₃⋯CO (**1**) complex (see Table 3), in agreement with van der Veken and Sluyts's proposal. Therefore, the tentative assignments carried out by these authors are fully supported on a theoretical basis.

In order to use the present theoretical approach also as a predictive tool, we explored the interaction energy hypersurface to locate the transition structures connecting the minima **1** (**1'**) and **2** (**2'**) experimentally detected (see Figure 2).²⁴ A Fourier transform microwave spectroscopy study might allow the estimation of the inversion barrier heights corresponding to the tunneling motions **1** → **1'** and **2** → **2'** (**TS1** and **TS2**; see Table 2) by determining the inversion splitting and using a one-dimensional-rotor Hamiltonian.²⁶ (The rotational constants *A* and *B* from the MP2/6-31G* calculations are 5.048 97, 1.709 54 and 5.058 64, 1.936 47 GHz for the BF₃⋯CO (**1**) and BF₃⋯OC (**2**) complexes, respectively. As can be observed, the experimental value of the rotational constant *B* for the BF₃⋯CO (**1**) complex as obtained from molecular beam electric resonance spectroscopy by Klemperer and co-workers² (1.64696 GHz) agrees reasonably well with the corresponding computed value.) Also, the dipole moments of the different structures, whose MP2/6-31G* values are given in Table 1, could be determined by Stark effect measurements (the computed dipole moments of the structures **1** and **5** point toward the oxygen atom of the CO molecule at the upper position—see Figure 1—while in the case of the structure **2**, the dipole moment points toward the carbon atom). As a matter of fact, the experimental dipole moment reported by Klemperer and co-workers² for the BF₃⋯CO (**1**) complex is 0.592 D, which agrees quite well with the computed value (0.795 D) bearing in mind the well-known difficulties associated with the precise theoretical estimate of

dipole moments.²⁷ The structural and energetic data provided in the present theoretical study²⁸ might be useful to analyze the results from the proposed spectroscopic study.

Regarding the 1:2 complexes, our extensive search on the interaction energy hypersurface yielded seven (**3**–**9**) minima structures (see Figure 1): two *D*_{3h} structures, one with the two carbon atoms of the two CO molecules pointing toward the boron atom of BF₃ (**3**) and the second one with the two oxygen atoms of the two CO molecules pointing toward the boron atom of BF₃ (**4**); one *C*_{3v} structure where the carbon atom of one of the two CO molecules and the oxygen atom of the second CO molecule are both pointing toward the boron atom of BF₃ (**5**); finally, four *C*_s structures where, besides the CO–BF₃ main interaction, there exists a significant CO–CO interaction as well (**6**–**9**). The MP4/6-31G**//MP2/6-31G* bond energies for these 1:2 complexes are given in Table 1. It is clear that the most stable structure is **3**, although, like in the case of the 1:1 complexes, some of the other structures should contribute to the infrared spectra. We hope that the structural and energetic data obtained in the present study for these complexes²⁸ might be useful to make further assignments. The experimental dissociation enthalpy for the OC⋯BF₃⋯CO complex as measured in liquefied argon⁵ (3.5 kcal/mol) is in between the theoretical (gas phase) uncorrected and CP-corrected values, which again agrees with the predicted overcorrection of the BSSE when using the CP method at the correlated level.²³ The experimental bond energy is closer to the CP-corrected values, especially at the MP2/aug-cc-pVDZ//MP2/D95* level of theory. On the other hand, the experimental bands⁵ at 643 and 1435 cm⁻¹ correlate quite well with the out-of-plane deformation (645 cm⁻¹) and antisymmetric stretching (1484 cm⁻¹) MP2/6-31G* vibrational frequencies obtained in the present study for the OC⋯BF₃⋯CO (**3**) complex (both vibrational frequencies are slightly lower than the corresponding ones, 666 and 1488 cm⁻¹, for the BF₃⋯CO (**1**) complex, in agreement with the experimental measurements⁵).

Finally, we would like to make a short comment on the nature of the interactions in the complexes dealt with in this paper, focusing on the differences between the BF₃⋯CO (**1**) and BF₃⋯OC (**2**) structures as resulting from NEDA¹⁵ and ANACAL^{17,19} analyses. Results from NEDA¹⁵ (HF/6-31G**//MP2/6-31G*) clearly indicate that charge transfer makes an important contribution to the stabilization of these two complexes. Indeed, the charge transfer and electrostatic components are –13.4 and –11.0 kcal/mol, respectively, for BF₃⋯CO (**1**) and –6.0 and –8.3 kcal/mol, respectively, for BF₃⋯OC (**2**) (deformation contributions partly counterbalance these stabilizing contributions to yield the final bond energies).¹⁵

To analyze in more detail the nature of the charge transfer process in these complexes,¹⁶ we used ANACAL¹⁷ (HF/6-31G**//MP2/6-31G*). The contribution of the zero configuration to the wave function of the complex according to ANACAL is in both cases very large (*c*₀ in eq 2 is 0.956 and 0.987 for BF₃⋯CO (**1**) and BF₃⋯OC (**2**), respectively) in agreement with the small bond energies reported in Table 1. In the case of the BF₃⋯CO (**1**) complex, the most significant contributions to the wave function come from the HOMO(CO) → LUMO(BF₃)

TABLE 3: Symmetric Stretching (ν_1), Out-of-Plane Deformation (ν_2), Antisymmetric Stretching (ν_3), and F–B–F Bending (ν_4) MP2/6-31G* Vibrational Frequencies (cm⁻¹) and IR Intensities (kcal/mol; in Brackets) for the Most Relevant Species

species	ν_1	ν_2	ν_3	ν_4
CO (<i>C</i> _{∞v})	2119 (σ_g) [25.8]			
BF ₃ (<i>D</i> _{3h})		699 (<i>a</i> _{2v}) [100.8]	1497 (<i>e'</i>) [409.3]	481 (<i>e'</i>) [12.8]
1 (<i>C</i> _{3v})	882 (<i>a</i> ₁) [1.8]	666 (<i>a</i> ₁) [185.5]	1488 (<i>e</i>) [376.3]	482 (<i>e</i>) [12.0]
2 (<i>C</i> _{3v})	887 (<i>a</i> ₁) [0.4]	685 (<i>a</i> ₁) [156.0]	1495 (<i>e</i>) [393.5]	482 (<i>e</i>) [11.0]
3 (<i>D</i> _{3h})		645 (<i>a</i> _{2v}) [272.6]	1484 (<i>e</i>) [347.4]	481 (<i>e'</i>) [9.5]

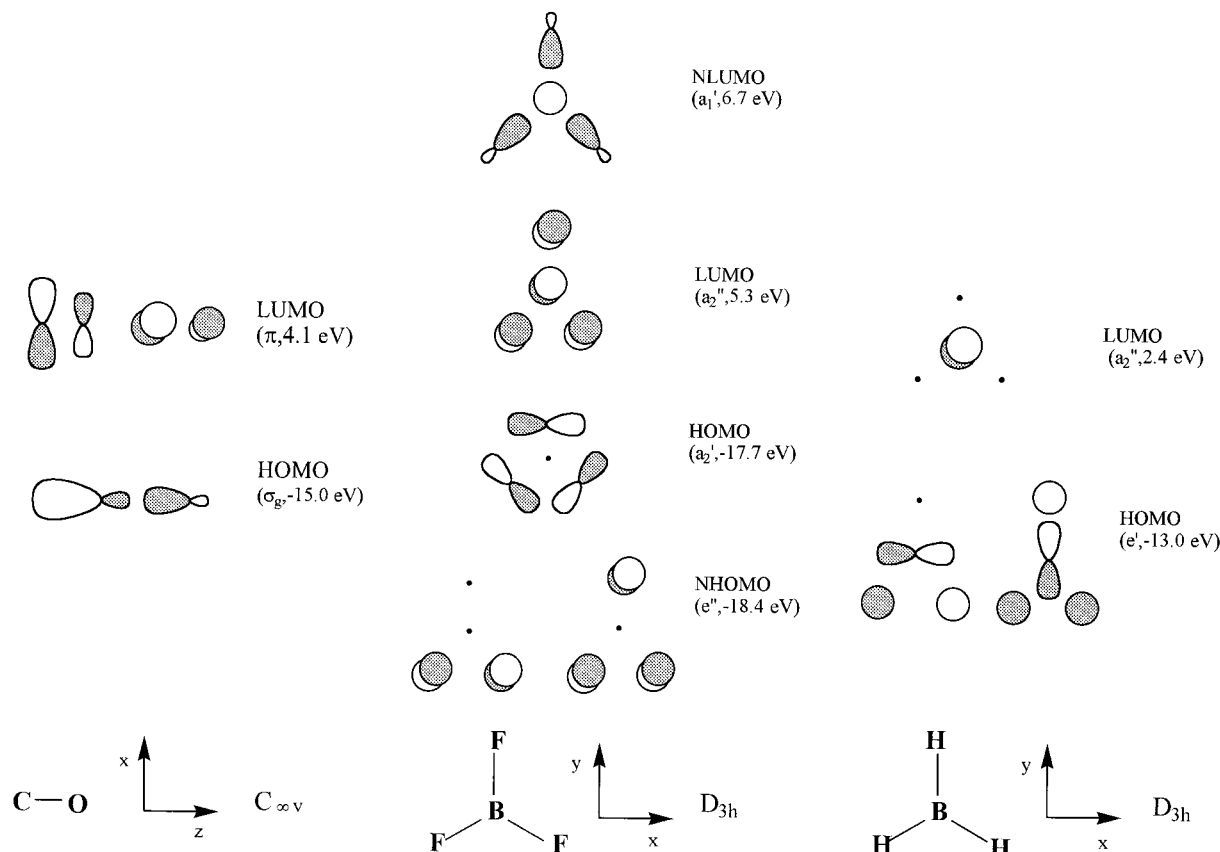


Figure 3. 6-31G** molecular orbitals close to the HOMO/LUMO region for BF_3 , BH_3 , and CO species. Molecular orbital energies are given in electronvolts.

($|c_r|^{29} = 0.064$), $\text{HOMO}(\text{CO}) \rightarrow \text{NLUMO}(\text{BF}_3)$ ($|c_r| = 0.034$) A^+B^- ($\text{A} = \text{CO}$, $\text{B} = \text{BF}_3$) monoterferred configurations, and $\text{NHOMO}(\text{BF}_3) \rightarrow \text{LUMO}(\text{CO})$ ($|c_r| = 0.019$) A^-B^+ (back-donation^{19c}) monoterferred configuration (it should be noted that the $\text{HOMO}(\text{BF}_3)$ doesn't have the appropriate symmetry; see Figure 3). The small charge transference, which correlates with the weak bond formed (see Table 1), can be ascribed to two main factors: (a) the large (~ 20 eV) HOMO – LUMO energetic separation (for the case of the $\text{BH}_3 \cdots \text{CO}$ complex, with a MP2/6-31G** bond energy of 24.8 kcal/mol, the HOMO – LUMO gap is ~ 17 eV) and (b) that the $\text{LUMO}(\text{BF}_3)$ and $\text{NLUMO}(\text{BF}_3)$ orbitals are antibonding between the boron atom and the fluorine atoms, and the $\text{NHOMO}(\text{BF}_3)$ is a pair of degenerate nonbonding orbitals completely localized on the fluorine atoms without any boron atom contribution (see Figure 3). Obviously, this situation is much less favorable than in the $\text{BH}_3 \cdots \text{CO}$ complex, with $\text{HOMO}(\text{CO}) \rightarrow \text{LUMO}(\text{BH}_3)$ ($|c_r| = 0.534$) A^+B^- ($\text{A} = \text{CO}$, $\text{B} = \text{BH}_3$) and $\text{HOMO}(\text{BH}_3) \rightarrow \text{LUMO}(\text{CO})$ ($|c_r| = 0.165$) A^-B^+ monoterferred configurations, where the $\text{LUMO}(\text{BH}_3)$ is a nonbonding p orbital completely localized on the boron atom, and the $\text{HOMO}(\text{BH}_3)$ is a pair of degenerate bonding orbitals which give rise to in-phase contributions with the $\text{LUMO}(\text{CO})$ pair of degenerate antibonding orbitals (see Figure 3).

The weaker nature of the bond in the case of the $\text{BF}_3 \cdots \text{OC}$ (2) complex is clearly attributable to the smaller size of the oxygen-centered part of the HOMO and LUMO in CO (see Figure 3). Indeed, a smaller overlap with the corresponding orbitals in BF_3 and, consequently, a smaller charge transfer should be expected.³⁰ The coefficients $|c_r|^{29}$ for the $\text{HOMO}(\text{CO}) \rightarrow \text{LUMO}(\text{BF}_3)$, $\text{HOMO}(\text{CO}) \rightarrow \text{NLUMO}(\text{BF}_3)$ and $\text{NHOMO}(\text{BF}_3) \rightarrow \text{LUMO}(\text{CO})$ monoterferred configurations are 0.021, 0.017, and 0.008, respectively. All these facts are

consistent with the smaller bond energy computed for this complex as compared with that of the $\text{BF}_3 \cdots \text{CO}$ (1) adduct (see Table 1).

Conclusions

The interaction energy hypersurfaces corresponding to the $\text{BF}_3(\text{CO})_n$ ($n = 1, 2$) van der Waals complexes have been explored. Two minima structures corresponding to the 1:1 type of complexes and seven corresponding to the 1:2 ones were located. The most stable 1:1 adduct, with MP2/aug-cc-pVDZ//MP2/D95* and MP4/D95*/MP2/D95* bond energies of 3.5 and 3.2 kcal/mol, respectively (CP-corrected values: 1.6 and 0.7 kcal/mol), is a C_{3v} structure with the carbon atom of the CO molecule pointing toward the boron atom ($\text{BF}_3 \cdots \text{CO}$). The computed values of the geometrical parameters and dipole moment for this complex agree quite well with those obtained from molecular beam electric resonance spectroscopy. The most stable 1:2 adduct, with MP2/aug-cc-pVDZ//MP2/D95* and MP4/D95*/MP2/D95* bond energies of 6.4 and 6.5 kcal/mol, respectively (CP-corrected values: 3.1 and 1.3 kcal/mol), is a D_{3h} structure with the two carbon atoms of the CO molecules pointing toward the boron atom ($\text{OC} \cdots \text{BF}_3 \cdots \text{CO}$). These (gas phase) computed bond energies are consistent with the experimental dissociation enthalpies of the 1:1 and 1:2 complexes as measured in liquefied argon, which were found to be 1.8 and 3.5 kcal/mol, respectively.

The experimentally observed broad band at the low-frequency side of the out-of-plane deformation vibrational frequency of the BF_3 monomer agrees quite well with the 685 cm^{-1} MP2/6-31G* predicted band for the 1:1 $\text{BF}_3 \cdots \text{OC}$ complex. This fact, together with the MP2/aug-cc-pVDZ//MP2/D95* and MP4/D95*/MP2/D95* bond energies obtained, 2.1 and 2.2 kcal/mol, respectively (CP-corrected values: 0.5 and 0.2 kcal/mol), gives

theoretical support for the hypothesis of the formation of this species. Also, the very weak band at 879 cm⁻¹ detected in the infrared spectra of the mixed BF₃/CO solutions (absent in the infrared spectra of BF₃) nicely correlates with the 882 cm⁻¹ MP2/6-31G* computed band corresponding to the symmetric BF₃ stretching fundamental of the BF₃···CO complex. That result is in full agreement with the tentative assignments proposed by van der Veken and Sluyts. The rest of the bands experimentally observed for the BF₃···CO and OC···BF₃···CO complexes (out-of-plane deformation and antisymmetric BF₃ stretching) agree quite well with the corresponding MP2/6-31G* computed values.

Finally, a theoretical analysis of the wave function of the complexes shows that their weakness clearly correlates with the very small charge transfers detected, which in turn can be ascribed to the large HOMO–LUMO gap and to the relative unsuitability of the orbitals closer to the HOMO/LUMO region. The weaker nature of the BF₃···OC complex as compared with the BF₃···CO one is clearly related to the smaller size of the oxygen-centered part of the HOMO and LUMO in the CO molecule.

References and Notes

- (1) *Van der Waals Interactions*, *Chem. Rev.* **1988**, *88*, 813–988. *Van der Waals Molecules*, *Chem. Rev.* **1994**, *94*, 1721–2160.
- (2) Janda, K. C.; Bernstein, L. S.; Steed, J. M.; Novick, S. E.; Klemperer, W. *J. Am. Chem. Soc.* **1978**, *100*, 8074.
- (3) Gebicki, J.; Liang, J. *J. Mol. Struct.* **1984**, *117*, 283. Lee, G.-H.; Takami, M. *J. Chem. Phys.* **1993**, *98*, 3612. Lee, G.-H.; Takami, M. *J. Mol. Struct.* **1995**, *352–53*, 417.
- (4) Jonas, V.; Frenking, G.; Reetz, M. T. *J. Am. Chem. Soc.* **1994**, *116*, 8741.
- (5) Sluyts, E. J.; van der Veken, B. J. *J. Am. Chem. Soc.* **1996**, *118*, 440.
- (6) Jonas, V.; Frenking, G. *J. Chem. Soc., Chem. Commun.* **1994**, 1489.
- (7) Fujiang, D.; Fowler, P. W.; Legon, A. C. *J. Chem. Soc., Chem. Commun.* **1995**, 113.
- (8) Iglesias, E.; Sordo, T. L.; Sordo, J. A. *Chem. Phys. Lett.* **1996**, *248*, 179.
- (9) (a) Francl, M. M.; Pietro, W. J.; Hehre, W. J.; Binkley, J. S.; Gordon, M. S.; DeFrees, D. J.; Pople, J. A. *J. Chem. Phys.* **1982**, *77*, 3654. (b) Dunning, T. H., Jr. *J. Chem. Phys.* **1970**, *53*, 2823. (c) Huzinaga, S. *J. Chem. Phys.* **1965**, *42*, 1293. (d) Dunning, T. H., Jr. *J. Chem. Phys.* **1989**, *90*, 1007. Kendall, R. A.; Dunning, T. H., Jr.; Harrison, R. J. *J. Chem. Phys.* **1992**, *96*, 6796.
- (10) Sordo, T.; Barrientos, C.; Sordo, J. A. *Basis Sets in Structure, Interactions, and Reactivity*; Fraga, S., Ed.; Elsevier: Amsterdam, 1992; Part A, Chapter 9.
- (11) Boys, S. F.; Bernardi, F. *Mol. Phys.* **1970**, *19*, 553.
- (12) Sordo, J. A.; Sordo, T. L.; Fernández, G. M.; Gomperts, R.; Chin, S.; Clementi, E. *J. Chem. Phys.* **1989**, *90*, 6361.
- (13) Xantheas, S. S. *J. Chem. Phys.* **1996**, *104*, 8821.
- (14) Frisch, M. J.; et al. *GAUSSIAN 92*; Gaussian, Inc.: Pittsburgh, PA, 1992. Frisch, M. J.; et al. *GAUSSIAN 94*; Gaussian, Inc.: Pittsburgh, PA, 1995.
- (15) Glendening, E. D.; Streitwieser, A. *J. Chem. Phys.* **1994**, *100*, 2900.
- (16) Leopold, K. R.; Fraser, G. T.; Novick, S. E.; Klemperer, W. *Chem. Rev.* **1994**, *94*, 1807.
- (17) Menéndez, M. I.; Sordo, J. A.; Sordo, T. L. *J. Phys. Chem.* **1992**, *96*, 1185. López, R.; Menéndez, M. I.; Suárez, D.; Sordo, T. L.; Sordo, J. A. *Comput. Phys. Commun.* **1993**, *76*, 235.
- (18) Fujimoto, H.; Kato, S.; Yamabe, S.; Fukui, K. *J. Chem. Phys.* **1974**, *60*, 572.
- (19) See for example: (a) López, R.; Sordo, J. A.; Sordo, T. L. *J. Chem. Soc., Chem. Commun.* **1993**, 1751. (b) Assfeld, X.; González, J.; López, R.; Ruiz-López, M. F.; Sordo, J. A.; Sordo, T. L. *J. Comput. Chem.* **1994**, *15*, 479. (c) Suárez, D.; Assfeld, X.; Ruiz-López, M. F.; Sordo, T. L.; Sordo, J. A. *J. Chem. Soc., Chem. Commun.* **1994**, 1683. (d) Suárez, D.; González, J.; Sordo, T. L.; Sordo, J. A. *J. Org. Chem.* **1994**, *59*, 8058. (e) Suárez, D.; Sordo, T. L.; Sordo, J. A. *J. Org. Chem.* **1995**, *60*, 2848. (f) Suárez, D.; Sordo, J. A.; Sordo, T. L. *J. Phys. Chem.* **1996**, *100*, 13462.
- (20) Inagaki, S.; Fujimoto, H.; Fukui, K. *J. Am. Chem. Soc.* **1975**, *97*, 6108, and references therein.
- (21) Bader, R. W. *Chem. Rev.* **1991**, *91*, 893.
- (22) Sordo, J. A. *J. Chem. Phys.* **1997**, *106*, 6204.
- (23) Cook, D. B.; Sordo, T. L.; Sordo, J. A. *J. Chem. Soc., Chem. Commun.* **1990**, 185. Cook, D. B.; Sordo, J. A.; Sordo, T. L. *Int. J. Quantum Chem.* **1993**, *48*, 375. Pudzianowski, A. T. *J. Chem. Phys.* **1995**, *102*, 8029. Ford, J. A.; Sreele, D. *J. Phys. Chem.* **1996**, *100*, 19336. Süle, P.; Nagy, A. *J. Chem. Phys.* **1996**, *104*, 8524.
- (24) Because the standard *intrinsic reaction coordinate* (IRC)²⁵ technique did not work properly for the type of structures considered in this work (possibly due to numerical problems associated with their extreme weakness), the two minima connected by each transition structure were found by using the following strategy: An IRC calculation starting from a given transition structure immediately fails providing two (false) minima structures, one on each path downhill from the saddle point. A full optimization starting from each such “minima” led to the two true minima connected by the transition structure being considered.
- (25) Gonzalez, C.; Schlegel, H. B. *J. Phys. Chem.* **1989**, *90*, 2154. Gonzalez, C.; Schlegel, H. B. *J. Phys. Chem.* **1990**, *94*, 5523.
- (26) See for example: Tan, X.-Q.; Xu, L.-W.; Tubergen, M. J.; Kuczowski, R. L. *J. Chem. Phys.* **1994**, *101*, 6512.
- (27) Johnson, B. G.; Gill, P. M. W.; Pople, J. A. *J. Chem. Phys.* **1993**, *98*, 5612.
- (28) The full set of MP2/6-31G* and MP2/D95* (for structures 1-3) geometrical parameters and vibrational frequencies of all the structures located and characterized in the present study are available upon request.
- (29) The |c_r| coefficients are the absolute values of coefficients c_q in eq 2 relative to the zero configuration coefficient, c₀.
- (30) Klopman, G. *J. Am. Chem. Soc.* **1968**, *90*, 223. Salem, L. *J. Am. Chem. Soc.* **1968**, *90*, 543. Salem, L. *Ibid.* **1968**, *90*, 553.